Designed Carrier Gas UV Laser Ablation Sensitizers for Cationic UV Curable Coatings

*Zhigang Chen and Dean C. Webster**
Department of Coatings and Polymeric Materials
Center for Nanoscale Science and Engineering
North Dakota State University
1735 NDSU Research Park Drive, Fargo, ND 58105

Abstract

Designed carrier gas UV laser ablation sensitizers for cationic UV curable coatings were synthesized and proved to greatly enhance laser ablation efficiency of sensitized coatings. A series of "carrier gas" sensitizers were synthesized by reacting hydroxyl containing reactive diluents such as oxetane and polyester polyols with monomethyl oxalyl chloride or dimethyl oxalate; the oxalyl group is considered as "carrier gas" generating moiety. Furthermore, a UV absorbing chromophore, naphthalene, is either chemically bound to the oxalyl containing molecules or blended with the synthesized oxalyl containing compounds to observe any synergistic effect. The "carrier gas" sensitizers were added into a typical cationic UV curable formulation to form different sensitized coatings, which were then characterized by thermogravimetric analysis (TGA), real time FTIR (RTIR) and ablated by a 355 nm laser. The ablation vias were examined using an optical profiler and SEM (scanning electron microscopy). Compared to the control sample, the sensitized coatings were found to have similar thermal decomposition temperature and higher functional group conversion during photopolymerization. All of the sensitized coatings containing "carrier gas" sensitizers exhibited better UV laser ablation performance than the control, and the combination of naphthalene derivatives and oxalyl group gave an even better ablation result, suggesting a synergistic effect. The chemical combination of naphthalene with oxalyl group exhibited better ablation sensitization than their blend, suggesting a more efficient intramolecular laser energy utilization process.

1. Introduction

Laser ablation of polymeric materials is receiving more and more attention as a processing method due to its advantages in many potential applications such as for the fabrication of microfluidic devices[1] and microelectronic/optical parts,[2] polymer fuel in laser plasma thrusters etc..[3] The mechanism of laser ablation involves both pyrolysis (thermal decomposition) and photolysis (photochemical decomposition) of the material.[4] Photolysis is the preferred mechanism in terms of ablation resolution since the involvement of thermal process can lead to unwanted deviation from the optimum quality of the structure.[5] Cleaner, higher resolution laser ablation is made possible by advances in laser technology and novel material development. The use of an ultrashort pulse laser such as a femtosecond laser provides much higher ablation resolution due to the minimization of laser induced heat effects.[5-7] On the material side, new photopolymers have been designed and synthesized. For example, polymers containing the triazene group in the backbone have been synthesized. The photosensitive triazene group absorbs the incident laser energy and photochemically decomposes into gaseous N_2, causing the fracture

* Corresponding author: Phone: (701) 231-8709. Fax: (701) 231-8439. E-mail: dean.webster@ndsu.edu

of the polymer backbone; following which, the N_2 generated (called "carrier gas") ejects out of the ablation site with supersonic velocity, carrying away polymer fragments and ablation debris, resulting in cleaner, higher resolution ablation structure.[3,8] Polyestercarbonates have also been synthesized and ablated by a 308 nm Excimer laser. Because of their absorption at the incident laser wavelength and the gaseous photochemical decomposition products of ester group such as CO and CO_2, they were reported to be ablated faster and with a higher resolution of the ablated microstructure.[2] Cycloaliphatic epoxide based cationic UV curable coatings are ideal candidates for microelectronic packaging materials due to their advantages such as good electrical properties [9,10] and low shrinkage during UV curing.[11] Using a 355 nm laser to ablate through-vias in these UV cured coatings is an important processing step in the fabrication of multilayered flexible electronic devices, but few reports can be found on either the 355 nm laser ablation of polymers or the laser ablation of UV curable materials.

Previously in this lab, the 355 nm laser ablation performance of cationic UV cured coatings was successfully improved by incorporating ~ 1% wt of reactive sensitizers as an additive.[12] In our ongoing research aiming to further improve the UV laser ablation performance of these coatings, this additive approach was again adopted, because it was shown that such the addition of laser ablation sensitizers does not significantly change the basic coating properties.[12] In this report, we demonstrate the utilization of the "carrier gas" concept to design and synthesize novel UV laser ablation sensitizers, which greatly enhance the UV laser ablation performance of these coating materials.

2. Experimental Section

2.1 Materials

Cyracure™ UVR 6110 difunctional cycloaliphatic epoxide (3,4-epoxycyclohexylmethyl-3-4-epoxycyclohexane carboxylate, ECC), UVR 6000 oxetane diluent (3-ethyl-3-hydroxymethyl oxetane, OXT) and UVI 6974 photoinitiator (mixed triarylsulfonium hexafluoroantimonate salt in propylene carbonate, PI) were obtained from Dow Chemical Company. AMBERLYST® 21 ion-exchange resin with tertiary amine functionality (A21), THF (HPLC grade), triethylene amine (TEA), 1-naphthol (1-Na-OH), 2-naphthol (2-Na-OH), 9-anthracene methanol (A-OH), dimethyl oxalate (DMO), 1-naphthalene chloride (1-Na Cl) and mono-methyl oxalyl chloride (MOC) were obtained from Aldrich. Dendritic polyester polyol H20 (H) and P1000 (P) were obtained from Perstorp Polyols, Inc. The polyol P1000 is supplied in liquid form, which is comprised of H20 (solid material) diluted with a polyether type polyol, according to Perstorp. All materials were used as received.

2.2 Synthesis of designed carrier gas sensitizers and sensitized coating formulation

Scheme 1 shows the synthesis routes for designed carrier gas sensitizers and Table 1 shows their synthesis and purification details. Table 2 shows the nominal structures of the synthesized "carrier gas" laser ablation sensitizers.

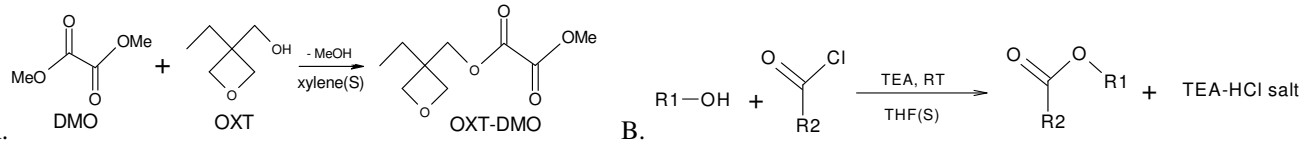

Scheme 1. Synthesis routes of carrier gas sensitizers: A) Synthesis of OXT-DMO by transesterification between OXT and DMO. B) Synthesis involving reaction of hydroxyl group and acid chloride. Where the R1-OH are polyols or 2-Na OH, and the acid chloride are MOC or 1-Na Cl.

Table 1. Synthesis detail for carrier gas sensitizers.

Sensitizer	Reactant ratio (mole)	Catalyst/ Neutralizer	Synthesis route & procedure	Purification	Characterization	Product appearance
OXT-DMO	OXT : DMO = 1:1	A21 (~10% wt of total reactants)	Scheme 1, route A. Charge reactants in a three neck round bottom flask, reaction under 100 °C in xylene for 12h w/magnetic stirrer, N_2 purge and water condenser	Vacuum (30 mm Hg) ~ 65 °C for 4.5h to remove the residual xylene and DMO	GC-MS	Viscous clear colorless liquid
Na-MOC	2-Na OH : MOC = 1:1.2	TEA (2-3 times the theoretical amount needed to neutralize the HCl generated during the reaction)	Scheme 1, route B. Charge reactants in a 20 ml glass vial w/THF, stir in water bath w/magnetic stirrer for ~ 10 min, charge TEA dropwise, then filter product solution using filter paper to remove the HCl-TEA salt.	Heat filtrate solution on hotplate ~100 °C w/N_2 purge ~ 30 min, followed by vacuum (30 mm Hg) 2-3 h at RT to remove the THF & TEA	GC-MS, UV-Vis	Deep brown solid
H-MOC	H : MOC = 1:8				FTIR, UV-Vis	Light yellow paste
P-MOC-Na	P : MOC : 1-Na Cl = 1:5:1				FTIR, UV-Vis	Light yellow clear paste
P-MOC	P : MOC = 1:5				FTIR, UV-Vis	Light yellow clear paste
P-Na	P : 1-Na Cl = 1:1				HPLC, FTIR, UV-Vis	Clear paste

Table 2. Nominal structures of synthesized "carrier gas" laser ablation sensitizers.

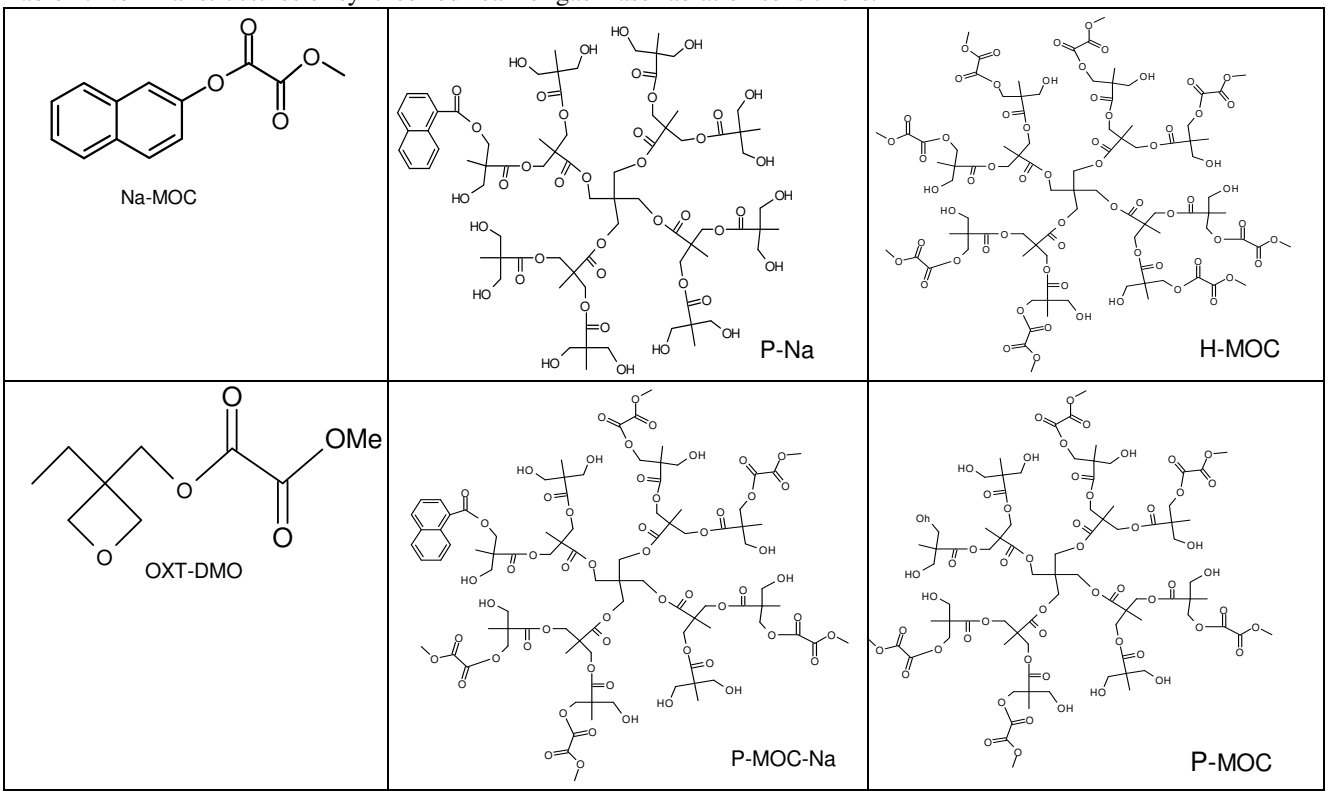

A series of sensitized coatings wre formulated in order to investigate the effect of carrier gas sensitizers. To avoid variation, a masterbase (MB) formulation (also serves as the control formulation) is

made and composed of 80% wt ECC, 16% wt OXT and 4% wt PI. This formulation was expected to be ablated with more difficulty due to its high T_g and crosslink density.[12] In using such a formulation it was hoped to differentiate the ablation sensitization performance between the sensitizers. Sensitizers were mixed into the MB formulation under slight heating (~ 50 °C) to make different sensitized coatings; the compositions are given in Table 3. In Table 3, except for OXT-DMO, all the other sensitizers were added at the ratio of 0.0001 mol per 5 g MB (if there are two sensitizers added, then each of them was added at the ratio of 0.0001 mol/5g MB; the theoretical molecular weight of the sensitizer were used for the calculations).

Table 3. Composition of the sensitized coating formulations studied in this work.

Formulations		Compositions		
Control		The Master Base (MB) - (80 wt% ECC, 16 wt% OXT, 4% wt PI		
CG-16		All of the OXT (16% wt) in MB are replaced by the reaction product in Scheme 1A		
CG-8		Half of the OXT (8 wt%) in MB are replaced by the reaction product in Scheme 1A		
CG-(A-OH)		+ A-OH	0.0208g	~ 0.42% wt
Group A	CG-(1-Na-OH)	+ 1-Na-OH	0.0144g	~ 0.29% wt
	CG-(Na-MOC)	+ Na-MOC	0.023g	~ 0.46% wt
	CG-(H-MOC)	+ H-MOC	0.2188g	~ 4.4% wt
	CG-(H-MOC+1-Na-OH)	+ H-MOC and 1-Na-OH	0.2188+0.0144g	~ 4.7% wt
Group B	CG-(P-MOC)	+ P-MOC	0.193g	~ 3.9% wt
	CG-(P-Na)	+ P-Na	0.1655g	~ 3.3% wt
	CG-(P-MOC+1-Na-OH)	+ P-MOC and 1-Na-OH	0.193+0.0144g	~ 4.1% wt
	CG-(P-MOC-Na)	+ P-MOC-Na	0.208g	~ 4.2% wt

2.3 Characterization

GC-MS analysis was performed on an HP 6890 gas chromatograph with an HP 5973 mass selective detector utilizing EI (electron ionization) with filament energy of 69.9 keV. The front inlet was in split mode with inlet temperature of 250 °C and pressure 8.24 psi., split ratio was 50:1. Initial GC oven temperature was 70 °C for 2 minutes, and then the temperature was ramped to 300 °C at a rate of 20 °C/min and was held for 16.5 minutes. Total run time was 30 minutes. Separation was achieved on a ZEBRON ZB-35 capillary column operated in a constant flow mode with flow rate of 1.0 ml/min., the average velocity was 36 cm/s. The mass spectrometer was in scan mode with m/z range from 10 to 800. The temperature for MS source and MS Quad were set at 230 °C and 150 °C respectively.

The FTIR and real time FTIR (RTIR) experiments were performed using a Nicolet Magna-IR 850 Spectrometer Series II with detector type DTGS KBr. For the RTIR experiments, a UV optic fiber was mounted in a sample chamber in which the humidity is kept around 20% by Drierite®. The light source was a LESCO Super Spot MK II 100W DC mercury vapor short-arc lamp. Such setup directly monitors the functional group conversion as the photo reaction proceeds. Coating samples were spin coated onto a KBr plate at 3000 rpm for about 15 s, which were then exposed to UV light for 60 s. Scans were taken over a 120 s period at 2 scans/s. The UV intensity was adjusted to ~3.6 mW/cm^2 and the experiment was performed in air. The oxirane conversion of ECC was monitored at 789 cm^{-1} and the oxetane conversion of EHMO was monitored at 976-977 cm^{-1}. The average conversion at 120 s is presented. The average standard deviation of this experiment is $\pm$ 2%.

Cured coating films were prepared by casting the liquid sample onto an aluminum panel (Q panel) with a Gardco 70# wire drawdown bar, followed by UV curing for 60 s in air using a Dymax

light source with a 200 EC silver lamp (UV-A, 365 nm). The intensity was ~35 mW/cm^2 measured by a NIST Traceable Radiometer, International Light model IL1400A. Cured coating films are ~80-100 µm thick measured by Micromaster® micrometer. The purpose of preparing such an unusually thick film is to monitor the laser ablation progress inside the coating film as the pulses increases. Free coating films were peeled off from aluminum panel using a razor blade for TGA analysis and laser ablation experiments.

UV laser ablation on cured coating films was done using a Continuum Surelite II Nd:YAG laser in a single shot mode. The laser beam passes through a Pellin-Brocca light prism into a Newport Model 935-5 attenuator, and then is focused on the sample surface using a Newport U-27X objective lens. Free coating films were taped on a ZAP-IT laser calibration panel and mounted on a 3D sample mount, the distance between the laser output and the sample film was 80 cm. The laser wavelength is 355 nm with beam spot size of approximately 40 µm, the pulse energy was adjusted to a lower value of ~0.93 mJ (measured using Molectron J9LP pyroelectric detector before lens) in order to better differentiate the sensitized samples. Each sample film was ablated under the same conditions and the ablation experiment was performed in air. Two rows of vias were ablated on each sample film as shown in Figure 1; vias in each row were ablated by 1, 2, 4, 8, 16 and 32 laser pulses, respectively, with the second row as a repetition of the first one. The via depth and volume data are based on the average value of these two identically ablated vias.

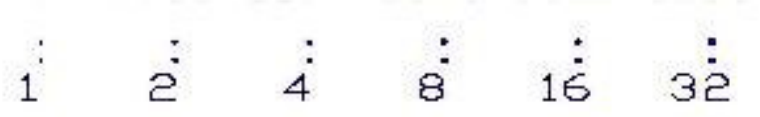

Figure 1. Ablated via array on coating film in UV laser ablation experiments.

Wyko NT3300 Optical Profiler from VEECO was used to obtain profile data of ablated vias. VSI (vertical scanning interferometry) mode and magnification of 50 × 0.5 were used. Back scan length was set at 15 µm, scan length was varied from 100 to 150 µm as pulses increases. Vision 32 for NT-2000 software, version 2.303 was used to process the dimension data for ablated vias. Scanning electron microscopy (SEM) images were obtained using a JEOL JSM-6300 Scanning Electron Microscope. Samples were mounted using carbon sticky tabs on aluminum mounts and coated with gold/palladium using a Balzers SCD 030 sputter coater.

UV-Vis spectra were obtained on a Varian Cary 5000 UV-Vis-NIR spectrophotometer operating in absorption mode. The scanning rate was 600 nm/min and scanning range was 200-600 nm. The compounds were dissolved in acetonitrile for the UV-Vis experiments. Thermogravimetric analysis (TGA) was performed using a TA Instruments TGA Q500 under nitrogen purging, the temperature was ramped from 25 °C to 650 °C at a ramping rate of 10 °C/min; the inflection point of the major degradation transition is presented as T_d.

3. Results and Discussion

3.1 Synthesis and effect of OXT-DMO - the first trial.

Since it is a novel approach to improve the UV laser ablation performance of cationic UV curable coatings using the concept of "carrier gas" laser ablation sensitizers, the need to design and tailor synthesize these sensitizer compounds is apparent. In the molecule design stage for these novel sensitizers, two key aspects were taken into consideration. The first one was the choice of the "carrier gas" generating functional group in the sensitizer molecule. Although nitrogen containing functional

groups such as triazene were reported to be effective in generating carrier gas (N_2) upon photolysis,[3,8] the basicity of such groups may inhibit the cationic photopolymerization of the oxirane and oxetane.[13] The oxalyl group was then chosen over the ester group as a good candidate for a "carrier gas" generating functional group due to its dense ester structure and the tendency to decompose into small molecule gases such as CO and CO_2. The second consideration was that it seems advantageous to chemically attach the oxalyl group to the monomers in the coating composition; thus the resulting sensitizer will have better compatibility with the coating matrix and any film property variation caused by migration will be eliminated. Based on these thoughts, synthesis was carried out to attach the oxalyl group to the hydroxyl oxetane monomer through the transesterification reaction as shown in Scheme 1A. The reaction product was named OXT-DMO, which formation was confirmed by GC-MS but with low yield (30% OXT-DMO, >50% OXT, and other minor impurities such as DMO). The other finding from the GC-MS result was that the oxalyl group will readily decompose and release desired gaseous fragments upon high energy input.

Though the content of OXT-DMO in the reaction product is low, nevertheless, it was incorporated into two coating formulations (CG-16 and CG-8). The other minor impurities such as DMO were not expected to have a major impact on coating properties. The coatings CG-16 and CG-8 were compared with control samples for a quick examination of OXT-DMO's effect on the three most important coating properties: UV curing behavior, thermal stability and laser ablation performance. The RTIR and TGA results are presented in Table 4. No major change was observed in the UV curing behavior and thermal stability of coatings after substituting the OXT with OXT-DMO.

Table 4. RTIR and TGA result of coatings with OXT-DMO in comparison with the control and A-OH sensitized coatings.

Formulations	RTIR 120s conversion (%)		T_d (°C)
	Epoxide	Oxetane	
Control	43	66	394
CG-16 (contains ~ 5% wt OXT-DMO)	48	62	393
CG-8 (contains ~ 2.4% wt OXT-DMO)	42	63	388
CG-(A-OH)	45	63	393

Table 5. Deepest ablated via depth (μm) for OXT-DMO containing coatings in comparison with the control and A-OH sensitized samples.

Pulses/Formula	Control	CG-16	CG-8	CG-(A-OH)
1	N	62.5, C	N	53.5, B
2	N	101.0, T	N	54.3, B
4	N		N	56.8, B
8	N		N	75.0, B
16	35.0, B		74.4, B	114.0, T

N=No ablation; B=Bulk material exists in the center of the hole as shown in Figure 2A; C=A clean hole is ablated as in shown in Figure 2B; T=A through hole ablated in the coating film.

The laser ablation data of these samples are given in Table 5, where letter "N" denotes no ablation, "T" denotes a through hole is ablated in the coating film, "B" stands for the scenario where bulk coating material still exists in the center of the hole while the surrounding material has been removed as illustrated in Figure 2A, and letter "C" denotes that a relatively cleaner hole is ablated as illustrated in Figure 2B. Here the ablation scenario graded by letter "B" is considered as a less efficient removal of material by laser ablation than the scenario graded by letter "C". The numbers in Table 5 are

the deepest via depth (in µm) data obtained from the "filtered histogram" analysis. The diameter of the ablated vias is around 30-50 µm.

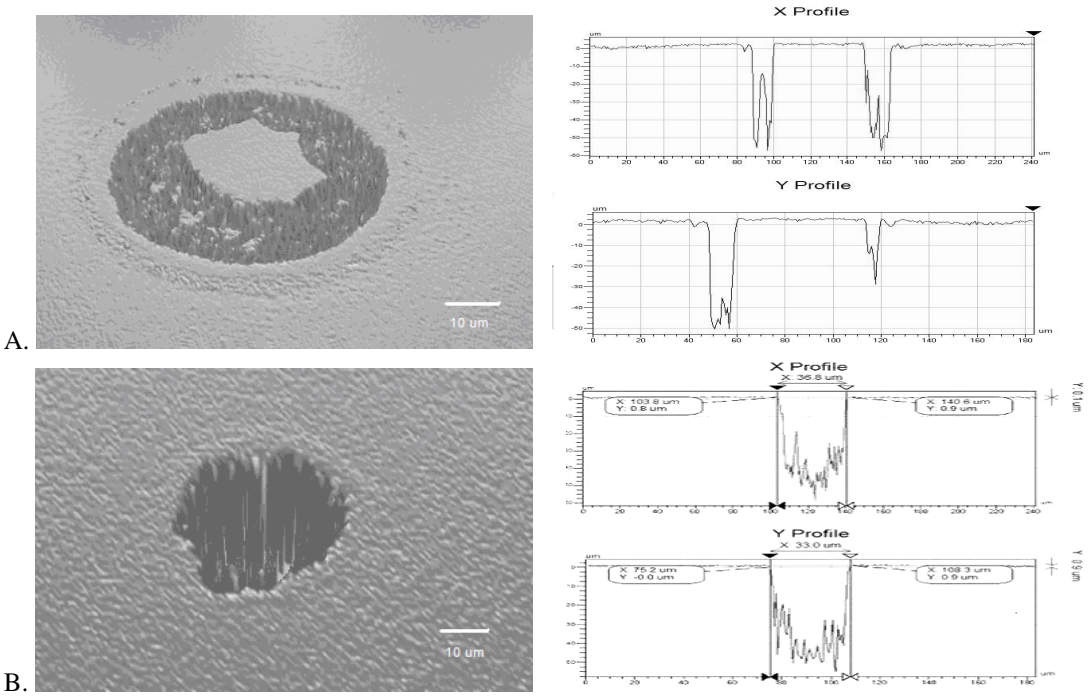

Figure 2. A. 3D and cross-section view of holes with materials remain in the center. B. 3D and cross-section view for a "cleaner" hole. Diameter of the via can be found from the cross-section view on the right.

From Table 5 it is apparent that the coating CG-16 has much better ablation result than all the other samples, especially the control and CG-8, for which the ablation starts only at 16 pulses. As to the coating CG-(A-OH), with the addition of anthracene methanol that absorbs at around 355 nm, its ablation starts as early as CG-16, but the removal of material is less complete. As laser pulses increase, the ablation depth for coating CG-(A-OH) increases and the central material bulk decreases in size due to laser ablation, but only at 16 pulses does the central bulk material completely disappear. These preliminary results suggest the efficacy of the "carrier gas" generating oxalyl group, however, it appears that a relatively large amount of OXT-DMO is needed to achieve better ablation. As to the difference observed between coating CG-(A-OH) and CG-16, it can be explained that the ablation of anthracene methanol and OXT-DMO sensitized samples are both based on the photothermal effect; but for the OXT-DMO containing films, the methyl oxalyl group may thermally decompose faster during the laser ablation process, and the released gaseous products can effectively eject more film material from the ablation site to create a cleaner hole.

3.2 Design, synthesis and characterization of "carrier gas" laser ablation sensitizers.

Though the initial UV laser ablation results after incorporating OXT-DMO are encouraging, the synthesis and purification of OXT-DMO is lengthy with low yield. On the other hand, it was thought that better laser ablation sensitization may be achieved with a sensitizer molecule having a 355 nm UV absorbing chromophore such as anthracene or naphthalene and the oxalyl groups chemically linked together. In this way the laser energy absorbed by the chromophore can be efficiently transferred to the oxalyl group intramolecularly, and consequently induce the decomposition of the oxalyl group into carrier gases either thermally or photochemically. It was also expected that if these two functional

groups are linked closely enough, they will synergistically respond to the incident laser energy and decompose photochemically, thus eliminating the energy loss during energy transfer process. So our subsequent synthesis efforts were focused on the design of sensitizer molecules embodying the above considerations. But the synthesis trials using transesterification and esterification routes were not promising, the reaction was lengthy under high reaction temperature, and the product was difficult to characterize and purify. Thus the hydroxyl - acid chloride reaction shown in Scheme 1B was chosen as an alterative. Using this chemistry, a series of "carrier gas" laser ablation sensitizers with UV absorbing chromophore and oxalyl group bound to the same molecule were systematically designed and synthesized. Table 1 describes the synthesis and purification details for these sensitizers, and Table 2 lists their nominal structures. Their characterization information is given below.

The molecular weight of Na-MOC is 230.22; its GC-MS analysis and UV-Vis spectrum are shown in Figure 3A and B respectively. In the GC chromatogram (left), the 9.73 min peak is unreacted 2-Na-OH, and the 11.80 min peak is Na-MOC. The MS spectrum of Na-MOC (right) shows its molecular ion peak m/z=230. The product contains > 80% Na-MOC. The UV-Vis spectrum of Na-MOC has more extended absorption (up to 400 nm) than that of naphthalene, which is the result of the linkage of two conjugated groups, the naphthalene and the oxalyl group. Consequently, Na-MOC not only has the naphthalene and oxalyl group directly bound to each other in one sensitizer molecule as desired, it also has the extra advantage of extended UV absorption covering the incident laser wavelength at 355 nm. The P-Na was synthesized in previous work in this lab, which purity is 95.5% as indicated by HPLC peak area integration.[14]

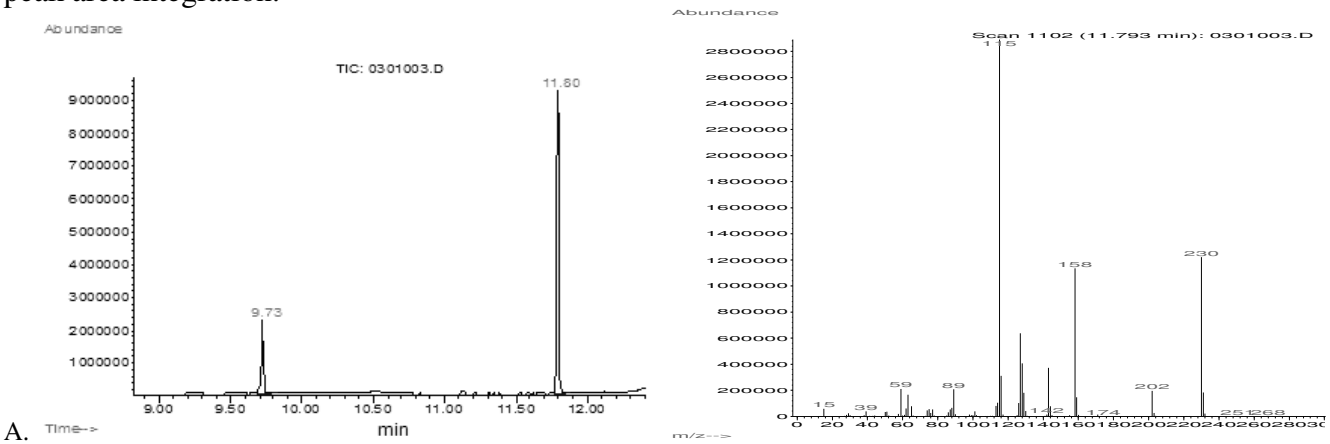

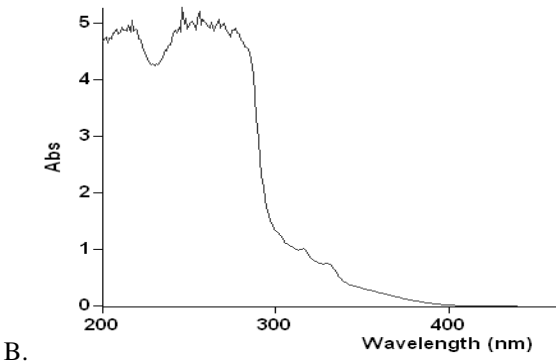

Figure 3. A. GC chromatogram (left) and MS spectrum (right) of Na-MOC. B. UV-Vis spectrum of Na-MOC.

For the synthesis of H-MOC, P-MOC and P-MOC-Na, the concept was to attach multiple oxalyl groups to one polyol molecule, so that a large amount of gaseous product will be generated upon decomposition of the sensitizer molecule. The dendritic polyester type polyol H and P proved to be the ideal starting materials for further chemical "decoration" due to their multiple hydroxyl functional groups (16 and 15 theoretical hydroxyl groups per molecule for polyol H and P respectively). The H-MOC, P-MOC and P-MOC-Na were characterized using FTIR and UV-Vis as shown in Figure 4 and Figure 5. Compared to the starting polyol P and H, a distinct feature in the FTIR spectra of these products is the decrease of the hydroxyl peak at 3300-3400 cm^{-1} and the increase of the carbonyl peak at ~1750 cm^{-1}, indicating the successful attachment of the oxalyl group. The UV-Vis spectra of these synthesis products (shown in Figure 5) are all different from the starting material H (or P), which has only a weak absorption around 250 nm. Also, it is noticed that after the attachment of naphthalene, as in the case of P-MOC-Na, the UV-Vis absorption of the sensitizer molecule is extended to around 350 nm.

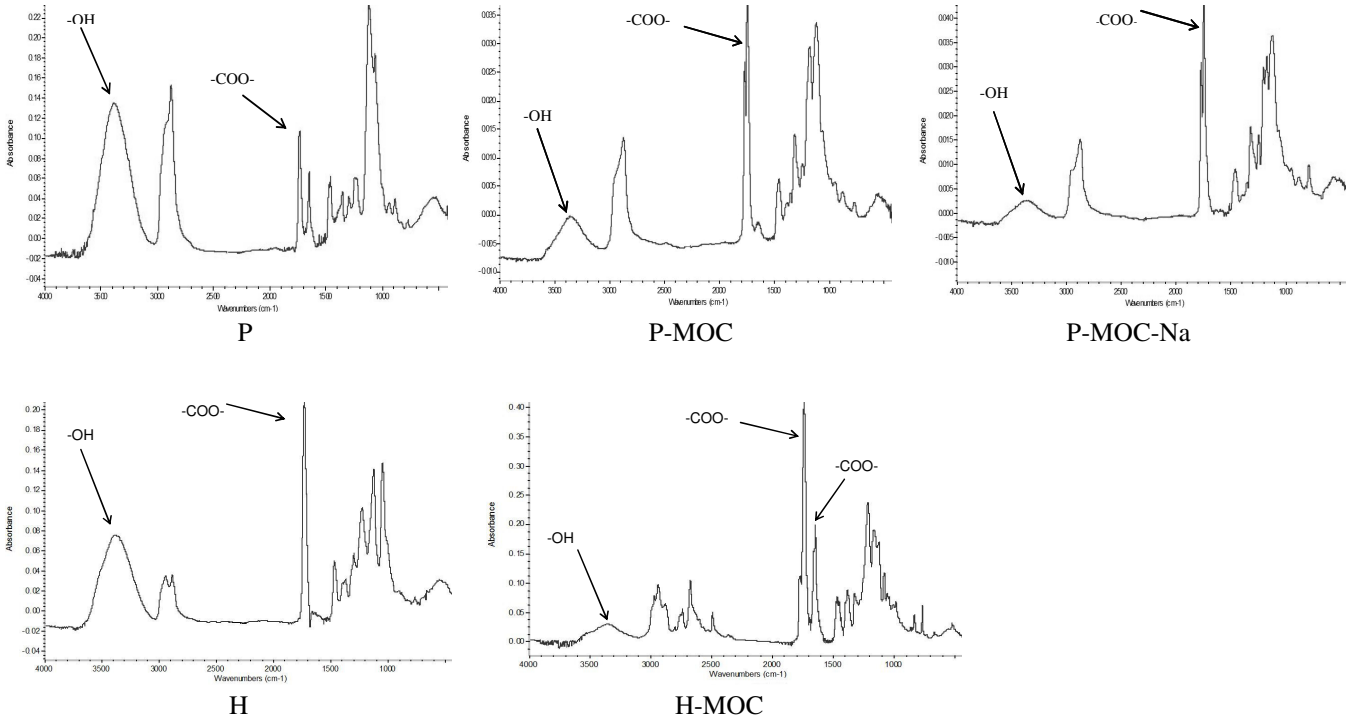

Figure 4. FTIR spectra of polyol H and P based "carrier gas" sensitizers.

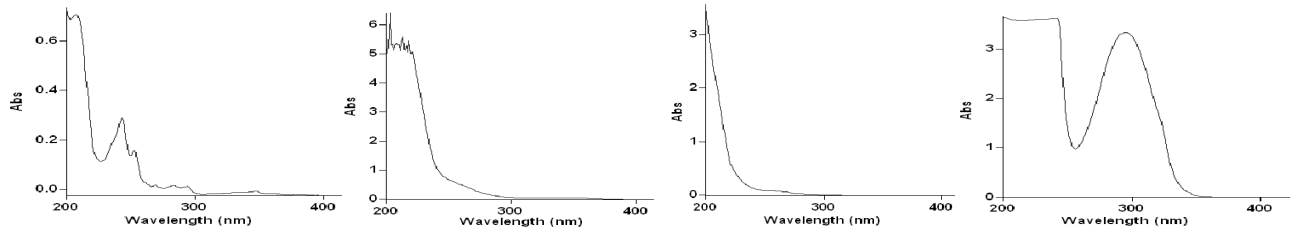

Figure 5. UV-Vis absorption spectra of polyol H and P based "carrier gas" sensitizers.

3.3 Effect of "carrier gas" laser ablation sensitizers.

The designed "carrier gas" sensitizers were added into the masterbase formulation to make different sensitized coatings, the addition percentage for them is ~ 3-5% wt for H and P based sensitizers and < 0.5% wt for the others. For better comparison, these formulations were arbitrarily divided into groups A and B as shown in Table 3. Group A includes coatings with H-based sensitizers and other formulations; Group B includes all coatings containing P-based sensitizers. These coatings together with the control sample were then characterized by RTIR and TGA followed by UV laser ablation to examine the effect of the added sensitizers.

The RTIR experiment results are shown in Table 6, where it can be seen that none of the sensitized coatings exhibit deterred UV curing compared to the control sample. A slight increase in reactive functional group conversion is observed after the addition of H-MOC or P-MOC while an appreciable increase in reactive functional group conversion after the addition of the naphthalene derivatives is noticed, which is attributed to their photosensitizing effect.[15-18] The extended UV absorption may account for the extraordinary photosensitizing effect of Na-MOC. It should also be noticed that when the naphthalene is chemically bound to a polyol species, the resultant sensitizer provides a much more pronounced photosensitization effect as can be seen in the case of P-Na and P-MOC-Na. This phenomena can be explained by the Intramolecular Hydrogen Abstraction Photosensitization mechanism as proposed previously,[14] while the even better photosensitization effect of P-MOC-Na than P-Na may due to the strengthened UV absorption of P-MOC-Na molecule contributed by the conjugated oxalyl groups. As to the thermal stability, TGA results in Table 6 show no significant change of T_d for sensitized samples as compared to control sample – all of the T_ds vary around 390 °C within a 15 °C range.

Table 6. Functional group conversion and thermal decomposition data for sensitized coatings in RTIR and TGA experiments.

Formulas/properties		Control (Master base)	Masterbase +							
			1-Na OH	Na-MOC	H-MOC	H-MOC+ 1-Na-OH	P-MOC	P-Na	P-MOC+ 1-Na-OH	P-MOC-Na
RTIR 120s conv. (%)	Epoxide	43	45	54	47	49	47	59	62	69
	Oxetane	57	65	71	65	68	61	81	79	82
TGA T_d (°C)		394	387	399	392	392	391	400	398	391

The variation in chemistry and molecular structure of the sensitizer molecules resulted in a significant difference in the UV laser ablation performance of sensitized coatings. Table 7 summarizes the via's deepest depth for group A and B coatings. The volume data of some better ablated vias in Group A and B were also obtained using the "multiple region analysis" tool in the Vision 32 software and is presented in Figure 6; this data is considered as a better representation of how well the hole is ablated.

Table 7. Deepest ablated via depth (μm) for group A and B sensitized coatings.

Pulses/Group A coatings	CG-(1-Na-OH)	CG-(Na-MOC)	CG-(H-MOC)	CG-(H-MOC+1-Na-OH)
1	B	55.1, B	44.9, B	55.6, C
2	55.9, B	76.3, C	54.3, B	56.3, C
4	39.5, B	113.5, T	68.2, C	79.2, C
8	63.0, B		105.5, T	104.0, T
16	94.0, T			
Pulses/Group B coatings	CG-(P-Na)	CG-(P-MOC-Na)	CG-(P-MOC)	CG-(P-MOC+1-Na-OH)
1	61.7, B	71.3, C	23.3, B	72.4, C
2	59.0, B	72.3, C	24.0, B	99.5, T
4	69.6, C	85.1, C	95.0, B	
8	124.0, T	85.3, C	103.0, T	
16		113, C		

N=No ablation; B=Bulk material exists in the center of the hole as shown in Figure 2A; C=Clean hole is ablated as in shown in Figure 2B; T=Through hole ablated in the coating film.

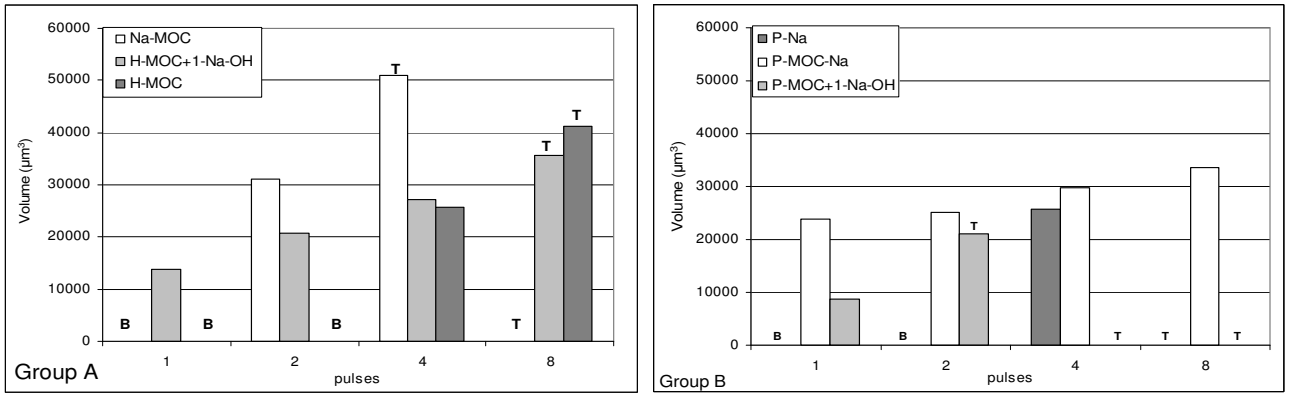

B=Bulk material exists in the center of the hole as shown in Figure 2A; T=A through hole ablated in the coating film.
Figure 6. Via volume data of some sensitized coatings.

From the ablation data in Table 7 and Figure 6, it is first noticed that the UV laser ablation performance of all sensitized samples is much better than the control sample for which ablation doesn't start until 16 pulses as shown in Table 4, while all the sensitized samples begin to be ablated within two pulses. For Group A coatings, in terms of laser ablation performance, they can be ranked in the following order (from better to worse): CG-(Na-MOC) > CG-(H-MOC+1-Na-OH) > CG-(H-MOC) > CG-(1-Na-OH). The addition of naphthalene derivative alone (CG-(1-Na-OH)) gives the least efficient removal of material at the ablation site; when carrier gas generation moiety is added (CG-(H-MOC)), a cleaner and deeper via than CG-(1-Na-OH) is achieved at 4 pulses. When both naphthalene and oxalyl groups are present in the formulation, as in the case of CG-(Na-MOC) and CG-(H-MOC+1-Na-OH), a synergistic effect that gives much better laser ablation can be observed: both formulations achieved a clean, deep hole within 2 laser pulses. A scenario can be envisioned to explain the better ablation of these two samples: the more "vulnerable" oxalyl functional group utilizes the energy absorbed by the laser energy absorber – naphthalene, either thermally or photochemically, and decomposes into carrier gases which then create a larger and cleaner via. Furthermore, by comparing the ablation data for coating CG-(Na-MOC) and CG-(H-MOC+1-Na-OH), it is noticed that the ablated holes of CG-(Na-MOC) are deeper and larger than that of CG-(H-MOC+1-Na-OH), so it seems the synergistic effect is more effective when the two functional groups – the naphthalene and the oxalyl group, are

chemically bound to each other than are just physically blended. The explanation for this is: For sensitizer Na-MOC, since its naphthalene and oxalyl group are directly linked to each other, it has more extended UV absorption than 1-Na-OH as a result of conjugation. What's more, it is very possible that the oxalyl group can directly utilize the absorbed laser energy by the whole Na-MOC molecule to decompose into carrier gases, so any energy loss during energy transport process is eliminated. The decomposition of Na-MOC is most probably a photochemical process. As to the physical blend of H-MOC and 1-Na-OH, a plausible energy utilization route is as follows: the absorbed laser photon energy is converted to thermal energy by naphthalene first, then transfers though the coating medium to H-MOC molecule and thermally decomposes it. This process is less efficient considering the loss during energy transportation. The other difference between coating CG-(Na-MOC) and CG-(H-MOC+1-Na-OH) is that the coating CG-(H-MOC+1-Na-OH) contains 7 times more oxalyl groups than CG-(Na-MOC). Also the polyol H in H-MOC brings in additional ester groups. The existence of a large amount of potential carrier gas generation moiety will definitely compensate for its less efficient energy utilization process during laser ablation of the coating, which may account for the difference observed at the first ablation pulse for these two formulations.

Sensitized coating samples from Group B are all polyol P based derivatives. Their ablation performance can be ranked as follows: CG-(P-MOC-Na) > CG-(P-MOC+1-Na-OH) > CG-(P-Na) > CG-(P-MOC). The effect of P-Na is better than 1-Na-OH and P-MOC, which may due to the fact that naphthalene is attached to a polyester polyol, so it is easier for the ester groups to intramolecularly utilize the absorbed laser energy by naphthalene to decompose and generate carrier gases, but such utilization may not be photochemical. The better laser ablation performance of CG-(P-MOC-Na) and CG-(P-MOC+1-Na-OH) was expected because of the decomposition tendency of oxalyl group and its synergistic effect with naphthalene as discussed earlier. Ablated vias of CG-(P-MOC-Na) are larger in volume than those of CG-(P-MOC+1-Na-OH); this may probably due to the more efficient intramolecular energy utilization process.

When comparing the best samples from Group A and B, it is found that the via volume for CG-(Na-MOC) is larger than that of CG-(P-MOC-Na), though they are all considered to have an intramolecular synergistic effect. But by envisioning the theoretical structure of P-MOC-Na as shown in Figure 7, such observation can be accounted for. The dendritic core of P-MOC-Na is polyol H, which is the main ingredient of polyol P. It has 8 branches with 16 hydroxyl groups on one molecule. For the synthesis of P-MOC-Na, the reactant ratio is P:MOC:1-Na Cl=1:5:1, so statistically naphthalene is still not that close to the oxalyl groups; subsequently the energy transfer will not be as facile and efficient as in Na-MOC. It is expected that if more oxalyl groups are attached, the intramolecular synergistic effect will be more pronounced. However, in spite of this, it is obvious that the combination of the carrier gas generation group and a UV absorber gives a much better laser ablation result.

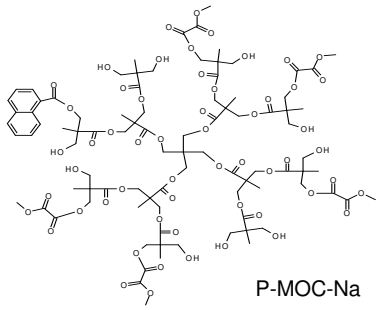

Figure 7. Theoretical structure of the "carrier gas" sensitizer P-MOC-Na.

SEM images were taken for some of the ablated vias as shown in Figure 8, which further corroborates the results obtained from the profiler. For CG-(1-Na-OH), even at 16 pulses, the material is not completely removed at the ablation site and it is apparent to see deposited ablation debris at and around the ablation site. The ablation of coating CG-(Na-MOC) at 2 pulses gives a cleaner material removal inside the via than the ablation of coating CG-(P-Na) at 4 pulses. In the second row of Figure 8, a more amazing scenario is observed. Even at 1 pulse, the ablation of coating CG-(P-MOC+1-Na-OH) and CG-(P-MOC-Na) gives a much cleaner ablated via than all of the other samples. These SEM images provide direct visual evidence that further confirm the effect of carrier gas sensitizers and the synergistic effect during laser ablation.

Though these synthesized novel "carrier gas" sensitizers exhibit a promising laser ablation enhancement effect, it is still desired to understand their decomposition mechanism upon laser energy. MALDI-TOF experiments are planned, and it is hoped that these results can provide more insight into the observations in this work.

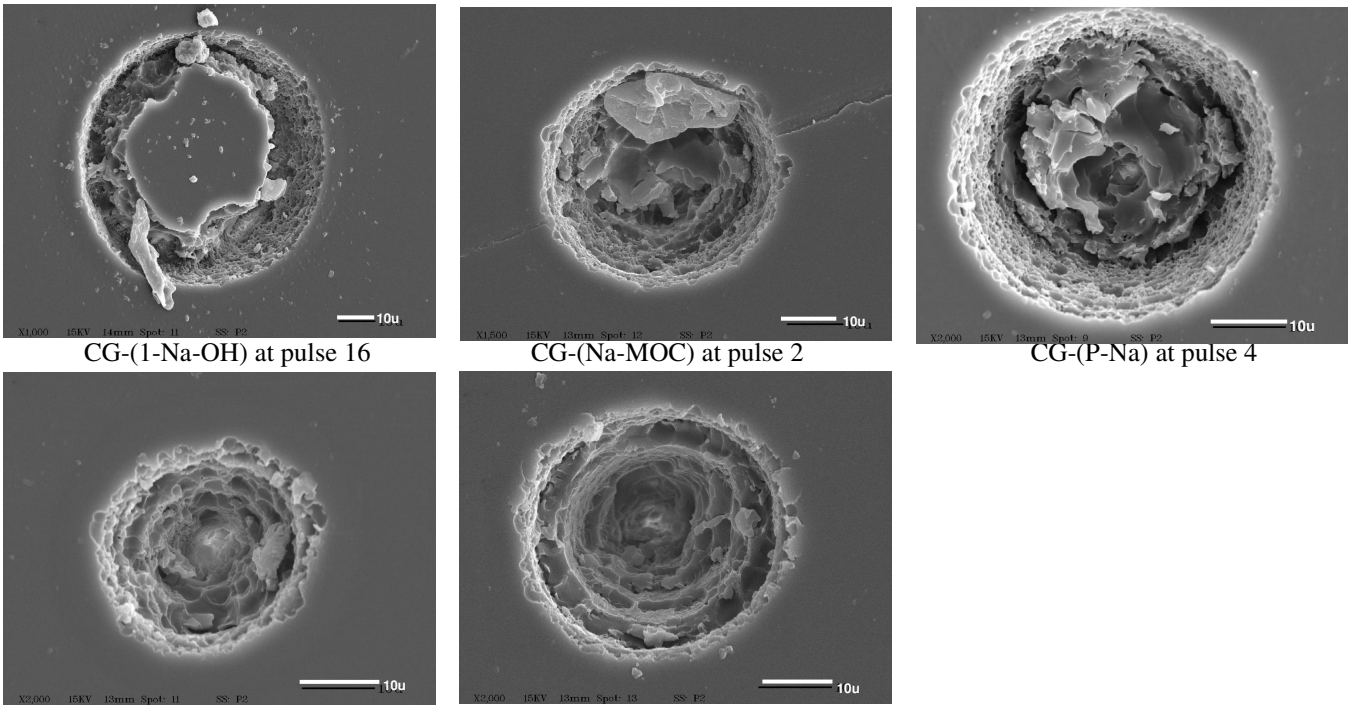

CG-(1-Na-OH) at pulse 16 CG-(Na-MOC) at pulse 2 CG-(P-Na) at pulse 4

CG-(P-MOC+1-Na-OH) at pulse 1 CG-(P-MOC-Na) at pulse 1

Figure 8. SEM images of some UV laser ablated vias.

Conclusions

A series of novel "carrier gas" laser ablation sensitizers were designed and synthesized by utilizing naphthalene as the UV laser energy absorber and oxalyl group as the carrier gas generator. These sensitizers were then characterized by GC-MS, HPLC, FTIR and UV-Vis. The synthesis and purification of OXT-DMO was difficult though enhanced laser ablation of a cationic UV curable coating was observed. The hydroxyl - acid chloride chemistry provides a facile, high yield route for the synthesis and purification of "carrier gas" sensitizers. Sensitizers were added into a masterbase formulation with the ratio of 0.0001 mol/5g masterbase to formulate different sensitized coatings. Compared to the control sample, the sensitized coatings exhibited no deterred UV curing and no significant change of thermal stability as revealed by RTIR and TGA, respectively, while optical profiler and SEM revealed that all the sensitized coating samples were much better ablated than the control in 355 nm laser ablation experiment. Furthermore, it was shown that the addition of naphthol or oxalyl modified polyols alone didn't greatly enhance the material removal during UV laser ablation either due to the thermal effect or lack of absorption of the laser energy. On the other hand, the combination of both naphthalene and oxalyl groups, either blended or, preferably, chemically bonded, showed a synergistic effect that results in much deeper, larger and cleaner ablated vias. One particular sensitizer, Na-MOC, with naphthalene and oxalyl group bound directly in one molecule, is especially effective considering its low addition level (< 0.5 % wt) and the resultant laser ablation enhancement. This result can be accounted for by Na-MOC's extended UV absorption and more efficient intramolecular utilization of the absorbed laser energy to generate carrier gases.

Acknowledgments

The authors thank the Center for Nanoscale Science and Engineering (CNSE) and the Defense Microelectronics Activity (DMEA) for support of this research under grant (DMEA 90-03-2-0303). We also thank Prof. Orven Swenson in Physics Department of NDSU for the help in laser ablation experiments and thank David Christianson and Shane Stafslien of CNSE for assistance with GC-MS and HPLC experiments.

References

(1) Pugmire D.L.; Waddell. E. A.; Haasch R.; Tarlov. M.J.; Locascio L. E. *Anal. Chem.* **2002**, *74*, 871-878.
(2) Kunz, T. S.; Stebani J.; Ihlemann, J.; Wokaun, A. *Appl. Phys. A,* **1998**, *67*, 347-352.
(3) Lippert, T.; Hauer, M.; Phipps, C. R.; Wokaun, A. A*ppl. Phys. A* **2003**, *77*, 259-264.
(4) Lippert, T. *Adv Polym Sci* **2004**, *168*, 51-246.
(5) Kruger, J. K.; Kautek W. *Adv. Polym. Sci.* **2004**, *168*, 247-289.
(6) Kruger, J. K.; Kautek W. *Applied Surface Science* **1996**, 96-98, 430-438.
(7) Serafetinides, A. A.; Makropoulou, M. I.; Skordoulis, C. D.; Kar, A. K. *Applied Surface Science* **2001**, *180*, 42-56.
(8) Nuyken, O.; Dahn, U.; Wokaun, A.; Kunz, T.; Hahn, C.; Hessel, V.; Landsiedel, J. *Acta Polym.* **1998**, *49*, 427-432.
(9) Koleske, J. V.; Spurr, O. K.; McCarthy, N. J. *National SAMPE Technical Conference* **1982,** 14, 249-256.
(10) Koleske, J. V.; McCarthy, N. J.; Spurr, O. K. *National SAMPE Technical Conference* **1984,** 16, 529-536.
(11) Chen, J. X.; Soucek, M.D. *Journal of Coatings Technology* **2003**, *75*, 49-.
(12) Chen, Z.; Webster, D. C. Study of cationic UV curing and UV laser ablation behavior of coatings sensitized by novel sensitizers, *Polymer*, submitted.
(13) Jang, M. C.; Crivello, J.V. *Journal of Polymer Science: Part A: Polymer Chemistry* **2003**, *41*, 3056-3073.
(14) Chen, Z.; Webster, D.C.; "Novel intramolecular hydrogen abstraction photosensitizers (IHA-PS) for cationic UV curable systems"; Proceedings, Radtech North America; 2006.
(15) Crivello, J. V.; Jiang, F. *Chem. Mater.* **2002,** 14, 4858-4866.
(16) Nelson, E. W.; Carter, T. P.; Scranton, A. B. *Polymeric Materials Science and Engineering,* **1993,** 69, 363-364.
(17) Cho, J. D.; Kim, H. K.; Kim, Y. S.; Hong, J. W. *Polymer Testing* **2003,** 22, 633-645.
(18) Hua, Y.; Jiang, F.; Crivello, J. V. *Chem. Mater.* **2002,** 14, 2369-2377.